Analysis of Oversampling in Uplink Massive MIMO-OFDM with Low-Resolution ADCs

Mengyuan Ma, Nhan Thanh Nguyen, Italo Atzeni, and Markku Juntti

Centre for Wireless Communications (CWC), University of Oulu, Finland

Email: {mengyuan.ma, nhan.nguyen, italo.atzeni, markku.juntti}@oulu.fi

Abstract—Low-resolution analog-to-digital converters (ADCs) have emerged as an efficient solution for massive multiple-input multiple-output (MIMO) systems to reap high data rates with reasonable power consumption and hardware complexity. In this paper, we analyze the performance of oversampling in uplink massive MIMO orthogonal frequency-division multiplexing (MIMO-OFDM) systems with low-resolution ADCs. Considering both the temporal and spatial correlation of the quantization distortion, we derive an approximate closed-form expression of an achievable sum rate, which reveals how the oversampling ratio (OSR), the ADC resolution, and the signal-to-noise ratio (SNR) jointly affect the system performance. In particular, we demonstrate that oversampling can effectively improve the sum rate by mitigating the impact of the quantization distortion, especially at high SNR and with very low ADC resolution. Furthermore, we show that the considered low-resolution massive MIMO-OFDM system can achieve the same performance as the unquantized one when both the SNR and the OSR are sufficiently high. Numerical simulations confirm our analysis.

Index Terms—Massive MIMO-OFDM, energy efficiency, low-resolution ADCs, oversampling.

I. Introduction

Massive multiple-input multiple-output (MIMO) is a crucial physical-layer technology for current and future wireless systems [1], which provides high spectral efficiency thanks to the large number of antennas at the base station (BS) [2]. However, when massive MIMO is adopted at millimeter wave and (sub-)THz frequencies [3], [4], its energy efficiency can be severely burdened by the high power consumption of each radio-frequency (RF) chain. In this respect, analog-to-digital converters (ADCs) are the most power-hungry RF components, as their power consumption increases exponentially with the number of resolution bits [5]. For instance, high-speed ADCs (e.g., operating at 1 Gsample/s) with high resolution (e.g., 8–12 bits) can consume several Watts [6]. Therefore, adopting low-resolution ADCs at the BS has been regarded as an effective approach to reducing power consumption without excessively compromising the performance [7], [8].

Despite the reduced power consumption, low-resolution ADCs introduce a non-linear quantization distortion to the signal, which cannot be eliminated by increasing the transmit power. While adding more antennas at the BS can compensate for the performance loss due to the quantization distortion [9]–[11], it also raises the overall power consumption and hardware complexity. On the other hand, temporal oversampling can improve the sum rate in quantized massive MIMO systems without increasing the number of antennas and RF chains [12].

Furthermore, oversampling enables higher-order modulation over a 1-bit quantized single-antenna additive white Gaussian noise (AWGN) channel [13]. In addition, it was shown in [14] that the sum rate grows roughly logarithmically with the oversampling ratio (OSR). Most of the aforementioned studies consider narrowband or single-carrier systems and are not readily applicable to wideband multi-carrier scenarios in general. This is because the correlation of time-domain symbols due to the low-resolution ADCs makes the frequency-domain signal model for multi-carrier systems more involved [15]. Massive MIMO orthogonal frequency-division multiplexing (MIMO-OFDM) systems with low-resolution ADCs and oversampling were studied by Üçüncü *et al.* in [16] under adjacent channel interference (ACI). Specifically, this work analyzed the performance with zero-forcing (ZF) combining and showed that oversampling can improve the signal-to-interference-plus-noise-and-distortion ratio (SINDR) and suppress the ACI in both 1-bit and multi-bit quantized systems.

Inspired by [16], we perform a deeper analysis of how the OSR, the ADC resolution, and the SNR collectively affect the performance of uplink massive MIMO-OFDM systems with low-resolution ADCs and oversampling, which was not reported in [16]. We first present the frequency-domain signal model for an uplink MIMO-OFDM system, which accounts for the impact of low-resolution ADCs on the received time-domain symbols. We then derive an approximate closed-form expression of an achievable sum rate based on the Bussgang decomposition, which considers the temporal and spatial correlation of the quantization distortion. Our analysis reveals that oversampling can significantly improve the sum rate by mitigating the quantization distortion, especially at high SNR and with very low ADC resolution (down to 1-bit). We further demonstrate that the considered low-resolution massive MIMO-OFDM system can achieve the same performance as its unquantized counterpart when both the SNR and the OSR are sufficiently high. Numerical simulations validate our analysis and highlight the trade-off between the OSR and the ADC resolution in terms of energy efficiency and hardware complexity.

II. System Model

We consider an uplink massive MIMO system where a BS equipped with M antennas receives signals from the U single-antenna user equipments (UEs). The OFDM is assumed over a wideband channel to deal with the frequency selectivity.

Specifically, let $\Delta f = \frac{1}{T_u}$ be the subcarrier spacing, where the OFDM symbol duration T_u is assumed to be fixed. Let $f_k = f_c + \left(k + 1 - \frac{N_c+1}{2}\right)\Delta f$, $k = 0, \ldots, N_c - 1$ denote the k-th subcarrier frequency, where f_c is the center carrier frequency. Among the total N_c subcarriers, K subcarriers are employed for signal transmission, while other $N_c - K$ subcarriers are employed for oversampling [15]. Let $\tilde{s}_u[k]$ be the transmit symbol of the u-th UE at subcarrier k with $\mathbb{E}\left[|\tilde{s}_u[k]|^2\right] = 1$, $k = 0, \ldots, K - 1$. Note that $\tilde{s}_u[k] = 0$ for $k = K, \ldots, N_c - 1$ when $N_c > K$. Because the sampling frequency is $f_s = N_c \Delta f$ while the transmission bandwidth of signals is $B_w = K\Delta f$, the OSR is defined as $\beta = \frac{N_c}{K}$. Hence, $\beta = 1$ and $\beta > 1$ indicate the Nyquist sampling and the oversampling scheme, respectively. The time-domain symbol is obtained by N_c-points inverse discrete Fourier transform (IDFT), which can be expressed as

$$s_u[n] = \frac{\sqrt{p}}{\sqrt{N_c}} \sum_{k=0}^{N_c-1} \tilde{s}_u[k] e^{j\frac{2\pi nk}{N_c}}, \quad n = 0, \ldots, N_c - 1, \quad (1)$$

where n represents the index of the time-domain symbol, and p denotes the average transmit power. At the receiver, the time-domain signals are first downconverted to the baseband and transformed back to the frequency domain by N_c-points discrete Fourier transform (DFT).

Let $\mathbf{s}[n] = [s_1[n], \ldots, s_U[n]]^T$ and $\tilde{\mathbf{s}}[k] = [\tilde{s}_1[k], \ldots, \tilde{s}_U[k]]^T$, where $\tilde{s}_u[k]$ is the frequency-domain signal transmitted by the u-th UE, and $s_u[n]$ is given in (1). The discrete-time received signal at time sample n at the BS is given by

$$\mathbf{r}[n] = \sum_{d=0}^{D-1} \mathbf{H}[d]\mathbf{s}[n-d] + \mathbf{w}[n], \quad (2)$$

where $D = \beta D_0$ with D_0 being the maximum number of delay taps under Nyquist sampling, and $\mathbf{H}[d] = [\mathbf{h}_1[d], \cdots, \mathbf{h}_U[d]] \in \mathbb{C}^{M \times U}$ denotes the channel matrix at the d-th time delay with $\mathbf{h}_u[d]$ representing the channel between the u-th UE and the BS. Here, $\mathbf{w}[n]$ represents the AWGN vector and $\mathbf{w}[n] \sim \mathcal{CN}(\mathbf{0}, \sigma_n^2\mathbf{I})$, where σ_n^2 denotes the AWGN power. By taking the DFT of both sides of (2), the frequency-domain received signal is expressed as

$$\tilde{\mathbf{r}}[k] = \sqrt{p}\tilde{\mathbf{H}}[k]\tilde{\mathbf{s}}[k] + \tilde{\mathbf{w}}[k], \quad k = 0, \ldots, N_c - 1, \quad (3)$$

where $\tilde{\mathbf{r}}[k] = \frac{1}{\sqrt{N_c}}\sum_{n=0}^{N_c-1} \mathbf{r}[n]e^{-j\frac{2\pi nk}{N_c}}$, $\tilde{\mathbf{w}}[k] = \frac{1}{\sqrt{N_c}}\sum_{n=0}^{N_c-1} \mathbf{w}[n]e^{-j\frac{2\pi nk}{N_c}}$, and $\tilde{\mathbf{H}}[k] = [\tilde{\mathbf{h}}_1[k], \ldots, \tilde{\mathbf{h}}_U[k]]$ with $\tilde{\mathbf{h}}_u[k] = \sum_{d=0}^{D-1} \mathbf{h}_u[d]e^{-j\frac{2\pi dk}{N_c}}$. Note that $\tilde{\mathbf{r}}[k] = \tilde{\mathbf{w}}[k]$ for $k = K, \ldots, N_c - 1$ as $\tilde{\mathbf{s}}[k] = \mathbf{0}$ in these cases.

III. Signal Model with Quantization

Assuming that the UEs employ high-resolution DACs, the BS uses identical pair of low-resolution ADCs in each RF chain for the in-phase and quadrature-phase signals. Focusing on the performance impact of ADCs, we assume in our analysis that all RF circuits other than the ADCs (e.g., local oscillators, mixers, and power amplifiers) are ideal. We further assume that the sampling rate f_s of the ADCs at the BS is the same as that of the DACs at the UE, and the system is perfectly synchronized. Finally, we assume that the spectrum of the output of ADCs is contained within $\left[-\frac{f_s}{2}, \frac{f_s}{2}\right]$, i.e., without out-of-band emissions [15].

A. Quantization Modeling

We begin by defining the codebook of a scalar quantizer of b bits as $\mathcal{C} = \{c_0, \ldots, c_{N_q-1}\}$, where $N_q = 2^b$ is the number of output levels of the quantizer. The quantization thresholds set is $\mathcal{T} = \{t_0, \ldots, t_{N_q}\}$, where $t_0 = -\infty$ and $t_{N_q} = \infty$ allows inputs with arbitrary power. For signals with standard Gaussian distribution, the Lloyd-Max algorithm can find the optimal $\mathcal{C}$ and $\mathcal{T}$ that achieve the minimum square error (MSE) between the input and output of the quantizer. Note that the Lloyd-Max quantizer is generally non-uniform, and the optimal $\mathcal{C}$ and $\mathcal{T}$ for 1–5 bits are given in [17, Table I]. Let $Q(\cdot)$ denote the quantization function. For a complex signal $x = \Re\{x\} + j\Im\{x\}$, we have $Q(x) = Q(\Re\{x\}) + jQ(\Im\{x\})$ with $Q(\Re\{x\}) = c_{I(\Re\{x\})}$, where $I(\Re\{x\}) = i \in \{0, \ldots, N_q - 1\}$ for $\Re\{x\} \in [t_i, t_{i+1}]$; $Q(\Im\{x\})$ is obtained in a similar way. When the input signal of the quantizer is a vector, $Q(\cdot)$ is applied elementwise.

The Bussgang decomposition allows to model a non-linear input-output relation of a Gaussian signal as a linear transformation [18]. To model the quantization of the received signal in (2) by the low-resolution ADCs, we first rewrite (2) as

$$\bar{\mathbf{r}} = \bar{\mathbf{H}}\bar{\mathbf{s}} + \bar{\mathbf{w}}, \quad (4)$$

where $\bar{\mathbf{r}} = \left[\mathbf{r}[N_c - 1]^T, \ldots, \mathbf{r}[0]^T\right]^T$, $\bar{\mathbf{s}} = \left[\mathbf{s}[N_c - 1]^T, \ldots, \mathbf{s}[0]^T\right]^T$, and $\bar{\mathbf{w}} = \left[\mathbf{w}[N_c - 1]^T, \ldots, \mathbf{w}[0]^T\right]^T$. Furthermore, $\bar{\mathbf{H}} \in \mathbb{C}^{MN_c \times UN_c}$ is a block circulant matrix [16]. With the Bussgang decomposition, $\bar{\mathbf{z}} = Q(\bar{\mathbf{r}})$ can be expressed as

$$\bar{\mathbf{z}} = \bar{\mathbf{B}}\bar{\mathbf{r}} + \bar{\boldsymbol{\eta}}, \quad (5)$$

where $\bar{\mathbf{z}} = \left[\mathbf{z}[N_c - 1]^T, \ldots, \mathbf{z}[0]^T\right]^T$, and where $\bar{\boldsymbol{\eta}} = \left[\boldsymbol{\eta}[N_c - 1]^T, \ldots, \boldsymbol{\eta}[0]^T\right]^T$ denotes the non-Gaussian distortion vector that is uncorrelated to $\bar{\mathbf{r}}$. Here, $\bar{\mathbf{B}}$ represents the Bussgang gain matrix. In the case of the same resolution (b bits) ADCs at all the RF chains, $\bar{\mathbf{B}}$ reduces to a scalar $\alpha = 1 - \gamma$, where γ denotes the inverse signal-to-quantization-distortion ratio (SQR). Note that, for a given resolution, γ is constant, which has been tabulated in [17]. Therefore, (5) is equivalent to

$$\mathbf{z}[n] = \alpha\mathbf{r}[n] + \boldsymbol{\eta}[n], \quad n = 0, \ldots, N_c - 1. \quad (6)$$

To facilitate the performance evaluation in the frequency domain, the analysis continues by taking the DFT of both sides of (6), yielding

$$\tilde{\mathbf{z}}[k] = \alpha\tilde{\mathbf{r}}[k] + \tilde{\boldsymbol{\eta}}[k]$$
$$= \alpha\sqrt{p}\tilde{\mathbf{H}}[k]\tilde{\mathbf{s}}[k] + \mathbf{e}[k], \quad k = 0, \ldots, N_c - 1, \quad (7)$$

where $\tilde{\mathbf{z}}[k] = \frac{1}{\sqrt{N_c}}\sum_{n=0}^{N_c-1} \mathbf{z}[n]e^{-j\frac{2\pi nk}{N_c}}$ and $\tilde{\boldsymbol{\eta}}[k] = \frac{1}{\sqrt{N_c}}\sum_{n=0}^{N_c-1} \boldsymbol{\eta}[n]e^{-j\frac{2\pi nk}{N_c}}$. Here, $\mathbf{e}[k] \triangleq \alpha\tilde{\mathbf{w}}[k] + \tilde{\boldsymbol{\eta}}[k]$ consisting of the AWGN and the quantization distortion is non-Gaussian due to $\tilde{\boldsymbol{\eta}}[k]$.

B. Achievable Sum Rate Analysis

Let $\mathbf{G}[k] = [\mathbf{g}_1[k], \ldots, \mathbf{g}_U[k]] \in \mathbb{C}^{M \times U}$ be the combining matrix of the k-th subcarrier at the BS. Thus, the post-

processing signal vector at subcarrier k is given by

$$\hat{\mathbf{x}}[k] = \mathbf{G}[k]^H \tilde{\mathbf{z}}[k] = \sqrt{p}\alpha \mathbf{G}[k]^H \tilde{\mathbf{H}}[k]\tilde{\mathbf{s}}[k] + \mathbf{G}[k]^H \mathbf{e}[k]. \quad (8)$$

The u-th element of $\hat{\mathbf{x}}[k]$ can be expressed as

$$\hat{x}_u[k] = \underbrace{\sqrt{p}\alpha \mathbf{g}_u[k]^H \mathbf{h}_u[k] s_u[k]}_{\text{desired signal}}$$

$$+ \underbrace{\sqrt{p}\alpha \sum_{j\neq u}^{U} \mathbf{g}_u[k]^H \mathbf{h}_j[k] s_j[k]}_{\text{interference}} + \underbrace{\mathbf{g}_u[k]^H \mathbf{e}[k]}_{\substack{\text{AWGN and}\\ \text{quantization}\\ \text{distortion}}}, \quad (9)$$

and the resulting SINDR is

$$\zeta_u[k] = \frac{p\alpha^2 |\mathbf{g}_u[k]^H \mathbf{h}_u[k]|^2}{p\alpha^2 \sum_{j\neq u}^{U} |\mathbf{g}_u[k]^H \mathbf{h}_j[k]|^2 + \mathbf{g}_u[k]^H \mathbf{C}_{\mathbf{e}_k} \mathbf{g}_u[k]}, \quad (10)$$

where $\mathbf{C}_{\mathbf{e}_k} = \mathbb{E}\left[\mathbf{e}[k]\mathbf{e}[k]^H\right] = \mathbf{C}_{\tilde{\boldsymbol{\eta}}_k} + \alpha^2 \sigma_{\mathrm{n}}^2 \mathbf{I}$ and $\mathbf{C}_{\tilde{\boldsymbol{\eta}}_k} = \mathbb{E}\left[\tilde{\boldsymbol{\eta}}[k]\tilde{\boldsymbol{\eta}}[k]^H\right]$. Treating the interference-plus-noise-and-distortion term as a Gaussian random variable with the same variance, we obtain an achievable sum rate as [9]

$$R = \sum_{k=1}^{K} \sum_{u=1}^{U} \Delta f \log_2\left(1 + \zeta_u[k]\right). \quad (11)$$

It is observed that $\mathbf{C}_{\tilde{\boldsymbol{\eta}}_k}$ is required to compute the sum rate in (11). However, obtaining $\mathbf{C}_{\tilde{\boldsymbol{\eta}}_k}$ may be challenging due to the quantization distortion. Alternatively, we derive an approximate closed-form expression in the following proposition.

Proposition 1 $\mathbf{C}_{\tilde{\boldsymbol{\eta}}_k}$ *can be approximated as*

$$\mathbf{C}_{\tilde{\boldsymbol{\eta}}_k} \approx \gamma(1-\gamma)\left(\frac{p}{N_{\mathrm{c}}} \sum_{k=0}^{K-1} \mathrm{diag}\left(\tilde{\mathbf{H}}[k]\tilde{\mathbf{H}}[k]^H\right) + \sigma_{\mathrm{n}}^2 \mathbf{I}\right), \quad (12)$$

where we recall that γ represents the inverse SQR given in [17], and p denotes the average transmit power. The approximation in (12) *becomes more accurate at low SNR or at high SNR with a low OSR and a high ADC resolution.*

Proposition 1 can be obtained through the DFT of the time-domain correlation matrix $\mathbf{C}_{\mathbf{r}}[\iota] = \mathbb{E}\left[\mathbf{r}[n]\mathbf{r}[n-\iota]^H\right]$ and $\mathbf{C}_{\boldsymbol{\eta}}[\iota] = \mathbb{E}\left[\boldsymbol{\eta}[n]\boldsymbol{\eta}[n-\iota]^H\right]$ as well as the approximation $\mathbf{C}_{\boldsymbol{\eta}}[0] \approx \gamma(1-\gamma)\mathrm{diag}(\mathbf{C}_{\mathbf{r}}[0])$ derived in [19]. The detailed proof is omitted due to limited space. Note that $\mathbf{C}_{\boldsymbol{\eta}}[\iota]$ includes the temporal and spatial correlations of the quantization distortion.

Using the result in (12), we can approximate $\mathbf{C}_{\mathbf{e}_k}$ as

$$\mathbf{C}_{\mathbf{e}_k} \approx (1-\gamma)\left(\frac{\gamma p}{N_{\mathrm{c}}} \sum_{k=0}^{K-1} \mathrm{diag}\left(\tilde{\mathbf{H}}[k]\tilde{\mathbf{H}}[k]^H\right) + \sigma_{\mathrm{n}}^2 \mathbf{I}\right). \quad (13)$$

From (13), the SINDR can be rewritten as

$$\zeta_u[k] \approx \frac{|\mathbf{g}_u[k]^H \mathbf{h}_u[k]|^2}{\sum_{j\neq u}^{U} |\mathbf{g}_u[k]^H \mathbf{h}_j[k]|^2 + \mathbf{g}_u[k]^H \mathbf{C}_{\mathbf{e}} \mathbf{g}_u[k]}, \quad (14)$$

where

$$\mathbf{C}_{\mathbf{e}} = \frac{\gamma}{(1-\gamma)\beta}\mathbf{H}_{\mathrm{e}} + \frac{1}{\rho(1-\gamma)}\mathbf{I} \quad (15)$$

with $\mathbf{H}_{\mathrm{e}} = \frac{1}{K}\sum_{k=0}^{K-1}\mathrm{diag}\left(\tilde{\mathbf{H}}[k]\tilde{\mathbf{H}}[k]^H\right)$ and $\rho = \frac{p}{\sigma_{\mathrm{n}}^2}$. Note that ρ denotes the SNR. We observe that the sum rate in (11)

based on (14) is jointly affected by three factors, i.e., the OSR, the ADC resolution, and the SNR. We note some important observations in the following:

1) With high ADC resolution, we have $\gamma \to 0$, which yields

$$\zeta_u[k] \to \frac{|\mathbf{g}_u[k]^H \mathbf{h}_u[k]|^2}{\sum_{j\neq u}^{U} |\mathbf{g}_u[k]^H \mathbf{h}_j[k]|^2 + \frac{1}{\rho}\|\mathbf{g}_u[k]\|^2}. \quad (16)$$

Based on (16), we can readily obtain the sum rate corresponding to the unquantized system.

2) It can be observed that increasing the OSR helps to mitigate the quantization distortion, which results in a higher sum rate. In particular, when the OSR increases without bound, i.e., $\beta \to \infty$, $\zeta_u[k]$ is limited by the SNR, which is

$$\zeta_u[k] \to \frac{|\mathbf{g}_u[k]^H \mathbf{h}_u[k]|^2}{\sum_{j\neq u}^{U} |\mathbf{g}_u[k]^H \mathbf{h}_j[k]|^2 + \frac{1}{\rho(1-\gamma)}\|\mathbf{g}_u[k]\|^2}. \quad (17)$$

This implies that, as the sum rate approaches the upper bound constrained by the SNR, the advantages gained from increasing the OSR become less significant.

3) In addition, at high SNR, oversampling can effectively improve the sum rate, especially with very low ADC resolution. In particular, when the SNR approaches infinity, i.e., $\rho \to \infty$, the second term of (15) approaches zero and $\mathbf{C}_{\mathbf{e}} \to \frac{\gamma}{(1-\gamma)\beta}\mathbf{H}_{\mathrm{e}}$. Hence, we obtain

$$\zeta_u[k] \to \frac{|\mathbf{g}_u[k]^H \mathbf{h}_u[k]|^2}{\sum_{j\neq u}^{U} |\mathbf{g}_u[k]^H \mathbf{h}_j[k]|^2 + \frac{\gamma}{\beta(1-\gamma)}\mathbf{g}_u[k]^H \mathbf{H}_{\mathrm{e}}\mathbf{g}_u[k]}, \quad (18)$$

which is limited by the quantization distortion and can be enhanced by increasing the OSR. Moreover, it is seen that a lower ADC resolution yields a larger $\frac{\gamma}{\beta(1-\gamma)}$, resulting in more significant performance enhancement due to oversampling. This is because γ is inversely proportional to the resolution and $\frac{\gamma}{1-\gamma}$ monotonically increases with γ. On the other hand, at low SNR, the benefits of increasing the OSR can be marginal because the second term of (15), i.e., the AWGN, could outweigh the quantization distortion.

4) When $\rho \to \infty$ and $\beta \to \infty$, we have

$$\zeta_u[k] \to \frac{|\mathbf{g}_u[k]^H \mathbf{h}_u[k]|^2}{\sum_{j\neq u}^{U} |\mathbf{g}_u[k]^H \mathbf{h}_j[k]|^2}, \quad (19)$$

which yields an upper bound of (16) when $\rho \to \infty$. This implies that, with sufficiently large SNR and OSR, a 1-bit quantized system can perform similarly to its unquantized counterpart.

We summarize the above discussions in the following remark:
Remark 1 *Oversampling can effectively improve the sum rate of low-resolution systems, especially at high SNR. In general, oversampling performs better at higher SNR and with lower ADC resolution. In particular, when both the SNR and the OSR are sufficiently large, the performance of the quantized system approaches that of the unquantized one.*

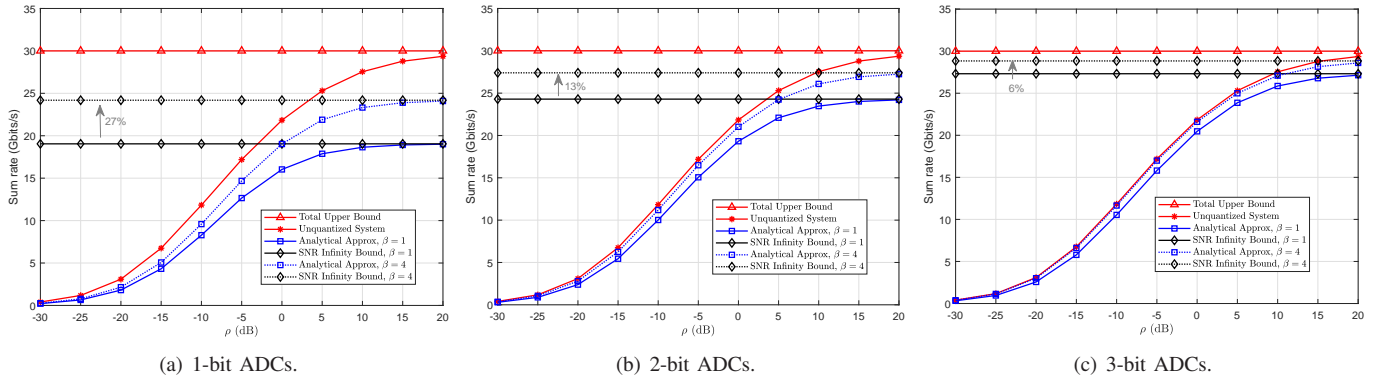(a) 1-bit ADCs.　　　　　　　　(b) 2-bit ADCs.　　　　　　　　(c) 3-bit ADCs.

Fig. 1. Achievable sum rate versus SNR with $M = 64$, $U = 4$, and $K = 128$.
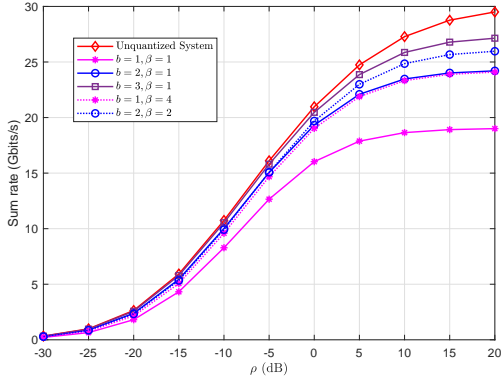

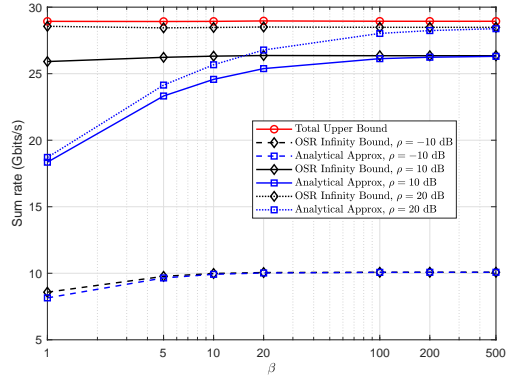Fig. 2. Achievable sum rate versus SNR with $M = 64$, $U = 4$, and $K = 128$.

Fig. 3. Achievable sum rate versus OSR with 1-bit ADCs, $M = 64$, $U = 4$, and $K = 128$.

IV. SIMULATION RESULTS

We consider the maximum ratio combining (MRC) to evaluate the achievable sum rate, which is $\mathbf{G}[k] = \mathbf{H}[k]\mathrm{diag}\left(\mathbf{H}[k]^H\mathbf{H}[k]\right)^{-1}$. The delay-$d$ channel between the u-th UE and the BS is modeled as [20]

$$\mathbf{h}_u[d] = \sqrt{\frac{M}{L}} \sum_{\ell=1}^{L} \beta_{u,\ell} p(dT_{\mathrm{s}} - \tau_{u,\ell})\mathbf{a}(\theta_{u,\ell}), \qquad (20)$$

where $\beta_{u,\ell}$, $\tau_{u,\ell}$, and $\theta_{u,\ell}$ denote the ℓ-th path gain, path delay and angle-of-arrival, respectively. Here, $p(t)$ represents the pulse-shaping function following the same parameters as in [20]. In the simulations, we assume $\beta_{u,\ell} \sim \mathcal{CN}(0,1)$, $\tau_{u,\ell} \sim \mathcal{U}\left[0, \frac{D_0}{B_{\mathrm{w}}}\right]$ with $D_0 = \frac{K}{4}$ as in [21], and $\theta_{u,\ell} \sim \mathcal{U}[0, 2\pi]$. Here, $\mathcal{U}[a,b]$ represents the uniform distribution in the interval $[a,b]$. The array steering vector is expressed as $\mathbf{a}(\theta) = \frac{1}{\sqrt{M}}\left[1, e^{-j\pi \sin(\theta)}, \ldots, e^{-j(M-1)\pi \sin(\theta)}\right]$. Furthermore, we set $f_{\mathrm{c}} = 140$ GHz, $\Delta f = 10$ MHz, $K = 128$, and $L = 3$ due to the channel sparsity in the (sub-)THz band. The AWGN power is $\sigma_{\mathrm{n}}^2 = N_0\Delta f$ with N_0 being the AWGN power density. The following results are obtained by averaging over 10^3 independent channel realizations.

Fig. 1 shows the achievable sum rate versus the SNR with 1-bit, 2-bit, and 3-bit ADCs. Specifically, we consider: (a) the sum rate obtained with $\rho \to \infty$ and $\beta \to \infty$ in (19) ("Total Upper Bound"); (b) the sum rate of the unquantized system in (16) ("Unquantized System"); (c) the approximate sum rate in (14) ("Analytical Approx"); and (d) the sum rate in (18)

obtained with $\rho \to \infty$ ("SNR Infinity Bound"). We make the following observations from these figures. First, increasing the ADC resolution leads to significant performance improvement, and employing 3-bit ADCs allows to approach the sum rate of the unquantized system. This agrees with the findings in [11]. Second, increasing the OSR substantially enhances the sum rate, especially at high SNR and with 1-bit ADCs, e.g., 27% and 6% performance improvement at $\rho = 20$ dB for the 1-bit and 3-bit quantized system, respectively. However, the performance improvement is marginal at low SNR cases due to the large AWGN. Third, it can be observed from Figs. 1(a) and 1(b) that the 1-bit quantized system with $\beta = 4$ can achieve a comparable sum rate to the configuration with 2-bit ADCs. However, since the typical power consumption of ADCs can be modeled as $\kappa f_{\mathrm{s}} 2^b$ with κ being the constant associated with the ADC quality [5], there is a trade-off between the OSR and the ADC resolution in terms of energy efficiency and hardware complexity.

Fig. 2 plots the achievable sum rate versus the SNR with different OSRs and ADC resolutions, where the power consumptions of ADCs are equated for three configurations based on $\kappa f_{\mathrm{s}} 2^b$, namely: (i) $b = 1$ and $\beta = 4$; (ii) $b = 2$ and $\beta = 2$; and (iii) $b = 3$ and $\beta = 1$. The results reveal that increasing the resolution of ADCs is more effective than increasing the OSR. Specifically, the configuration with $b = 3$ and $\beta = 1$ achieves the highest performance. Moreover, it is observed that the system that employs 1-bit ADCs oversampled by a factor

of 4 can attain comparable performance to the 2-bit system without oversampling. However, this comes at the cost of double the energy expenditure. This observation is consistent with the results reported in [16] regarding the bit error rate. Nonetheless, we remark that 1-bit quantized systems have very low hardware complexity (e.g., the automatic gain control used in multi-bit quantized systems is no longer needed), which is not taken into account in our numerical results.

Fig. 3 depicts the achievable sum rate versus the OSR with 1-bit ADCs. The sum rate obtained with (17) at $\beta \to \infty$ is referred to as "OSR Infinity Bound". It is seen that oversampling can substantially improve the sum rate at medium-to-high SNR, while it only yields minor benefits for low SNR scenarios. Furthermore, increasing the SNR and the OSR can progressively bridge the performance gap between the 1-bit quantized and the unquantized systems. This is due to the system performance being jointly corrupted by the AWGN and the quantization distortion. While improving the SNR can overcome the AWGN, the resulting reduced randomness makes the quantization distortion more significant. Therefore, oversampling, which mitigates the quantization distortion, can further enhance the system performance. As such, oversampling is more effective at high SNR, as observed in Fig. 3. Ideally, when $\beta \to \infty$, the quantization distortion can be entirely suppressed, and the performance is upper-bounded by the SNR. However, it is observed that, for $\beta \geq 20$, increasing the OSR yields only minor gains. Therefore, determining a reasonable OSR is crucial to achieve a suitable trade-off between sum rate and energy efficiency, considering that the power consumption of the ADCs increases linearly with the sampling frequency.

V. CONCLUSION

We analyzed the impact of oversampling on the achievable sum rate in an uplink massive MIMO-OFDM system with low-resolution ADCs. Both the analytical and numerical results demonstrated that oversampling can significantly improve the sum rate of quantized systems by mitigating the quantization distortion. In particular, oversampling gives higher gains at higher SNR and with lower ADC resolution (especially down to 1-bit). Furthermore, we showed that the system with low-resolution ADCs can approach the performance of the unquantized system when both the SNR and the OSR are sufficiently high. Moreover, the results indicate the necessity to strike a balance between the OSR and the ADC resolution in terms of energy efficiency and hardware complexity. We note that, although these results are obtained assuming single-antenna UEs, they can be similarly derived for the scenario with multi-antenna UEs. Furthermore, we observed similar results using ZF combining, with the difference being that higher sum rate improvements are achieved due to oversampling compared to employing MRC. Future research may investigate the trade-off between the OSR and the ADC resolution to maximize the energy efficiency.

REFERENCES

[1] N. Rajatheva, I. Atzeni, E. Björnson *et al.*, "White paper on broadband connectivity in 6G," http://jultika.oulu.fi/files/isbn9789526226798.pdf, 2020.

[2] M. A. Albreem, M. Juntti, and S. Shahabuddin, "Massive MIMO detection techniques: A survey," *IEEE Commun. Surveys Tuts.*, vol. 21, no. 4, pp. 3109–3132, 2019.

[3] E. Bjornson, L. Van der Perre, S. Buzzi, and E. G. Larsson, "Massive MIMO in sub-6 GHz and mmWave: Physical, practical, and use-case differences," *IEEE Wireless Commun.*, vol. 26, no. 2, pp. 100–108, 2019.

[4] A. Shafie, N. Yang, C. Han, J. M. Jornet, M. Juntti, and T. Kurner, "Terahertz communications for 6G and beyond wireless networks: Challenges, key advancements, and opportunities," *IEEE Netw.*, 2022.

[5] B. Murmann, "The race for the extra decibel: A brief review of current ADC performance trajectories," *IEEE Solid-State Circuits Mag.*, vol. 7, no. 3, pp. 58–66, 2015.

[6] Y. Li, C. Tao, G. Seco-Granados, A. Mezghani, A. L. Swindlehurst, and L. Liu, "Channel estimation and performance analysis of one-bit massive MIMO systems," *IEEE Trans. Signal Process.*, vol. 65, no. 15, pp. 4075–4089, 2017.

[7] J. Liu, Z. Luo, and X. Xiong, "Low-resolution ADCs for wireless communication: A comprehensive survey," *IEEE Access*, vol. 7, pp. 91 291–91 324, 2019.

[8] I. Atzeni and A. Tölli, "Channel estimation and data detection analysis of massive MIMO with 1-bit ADCs," *IEEE Trans. Wireless Commun.*, vol. 21, no. 6, pp. 3850–3867, 2022.

[9] L. Fan, S. Jin, C.-K. Wen, and H. Zhang, "Uplink achievable rate for massive MIMO systems with low-resolution ADC," *IEEE Commun. Lett.*, vol. 19, no. 12, pp. 2186–2189, 2015.

[10] C. Mollen, J. Choi, E. G. Larsson, and R. W. Heath, "Uplink performance of wideband massive MIMO with one-bit ADCs," *IEEE Trans. Wireless Commun.*, vol. 16, no. 1, pp. 87–100, 2016.

[11] S. Jacobsson, G. Durisi, M. Coldrey, U. Gustavsson, and C. Studer, "Throughput analysis of massive MIMO uplink with low-resolution ADCs," *IEEE Trans. Wireless Commun.*, vol. 16, no. 6, pp. 4038–4051, 2017.

[12] A. B. Üçüncü and A. Ö. Yılmaz, "Oversampling in one-bit quantized massive mimo systems and performance analysis," *IEEE Trans. Wireless Commun.*, vol. 17, no. 12, pp. 7952–7964, 2018.

[13] S. Krone and G. Fettweis, "Capacity of communications channels with 1-bit quantization and oversampling at the receiver," in *IEEE Sarnoff Symp.*, 2012, pp. 1–7.

[14] R. Deng, J. Zhou, and W. Zhang, "Bandlimited communication with one-bit quantization and oversampling: Transceiver design and performance evaluation," *IEEE Trans. Commun.*, vol. 69, no. 2, pp. 845–862, 2020.

[15] S. Jacobsson, G. Durisi, M. Coldrey, and C. Studer, "Linear precoding with low-resolution DACs for massive MU-MIMO-OFDM downlink," *IEEE Trans. Wireless Commun.*, vol. 18, no. 3, pp. 1595–1609, 2019.

[16] A. B. Üçüncü, E. Björnson, H. Johansson, A. Ö. Yılmaz, and E. G. Larsson, "Performance analysis of quantized uplink massive MIMO-OFDM with oversampling under adjacent channel interference," *IEEE Trans. Commun.*, vol. 68, no. 2, pp. 871–886, 2019.

[17] J. Max, "Quantizing for minimum distortion," *IRE Trans. Inf. Theory*, vol. 6, no. 1, pp. 7–12, 1960.

[18] J. J. Bussgang, "Crosscorrelation functions of amplitude-distorted Gaussian signals," Res. Lab. Electron., Massachusetts Inst. Technol., Tech. Rep., 1952.

[19] A. Mezghani and J. A. Nossek, "Capacity lower bound of MIMO channels with output quantization and correlated noise," in *Proc. IEEE Int. Symp. Inf. Theory*, 2012.

[20] A. Alkhateeb and R. W. Heath, "Frequency selective hybrid precoding for limited feedback millimeter wave systems," *IEEE Trans. Commun.*, vol. 64, no. 5, pp. 1801–1818, 2016.

[21] S. Park, A. Alkhateeb, and R. W. Heath, "Dynamic subarrays for hybrid precoding in wideband mmWave MIMO systems," *IEEE Trans. Wireless Commun.*, vol. 16, no. 5, pp. 2907–2920, 2017.